FLOW OVER CAVITIES IN TRANSONIC REGIME: A TEST CASE FOR NUMERICAL SIMIULATIONS

Nicolas Forestier, Philippe Geffroy, Laurent Jacquin
Fundamental and Experimental Aerodynamics Department, ONERA
29, avenue de la Division Leclerc, 92320 Châtillon - France

ABSTRACT

Two techniques were developed for characterizing the unsteady shear layer which develops on the open side of a deep cavity. The first is a 20 kHz spark light system (Nanolite/Strobokin) coupled with a rotating photographic apparatus (Strobodrum). The second is an acquisition method using a two-component Laser Doppler Velocimeter synchronized with the unsteady pressure measured in the cavity (Kulite sensor). This technique was used to determine phase averages by Lyn and Rodi's method (1994).

INTRODUCTION

The flow which develops above a cavity is a reference problem used for validating L.E.S. (Large Eddy Simulation) and D.N.S. (Direct Numerical Simulation) type unsteady numerical methods. Acquisition of precise unsteady data involving special processing is required to validate such methods.

Phenomenologically, an initial classification distinguishes between "open" cavities and "closed" cavities. Closed cavities are characterized by reattachment of the mixing layer to the bottom of the cavity. Length/depth (L/D) ratios above 10 are observed in this case (Sarohia (1977) demonstrated that the ratio could be decreased to 7 in the case of a laminar upstream boundary layer). There are two subcategories of open cavities: deep cavities (L/D<1) and shallow cavities (L/D>1). We investigated the case of a deep cavity with an aspect ratio L/D of 0.4.

Generally speaking, cavity flows are characterized by acoustic coupling between the upstream trailing edge where the boundary layer separates and the leading edge located downstream of the cavity where the mixing layer reattaches (Rockwell and Naudascher, 1979). This coupling or feedback mechanism was described several decades ago by Rossiter (1964). It is similar to the edgetone resonance mechanism described by Powell (1961). The unsteady features of the flow above an open cavity are entirely controlled by this acoustic feedback. This is explained by the following phenomena. An interface stability develops near the leading edge. It is convected and amplified to saturation. When this structure impinges on the downstream wall of the cavity, the resulting pressure disturbance is propagated into the cavity at a speed close to the speed of sound. This acoustic disturbance selects the dominant unstable mode in the upstream part of the mixing layer.

Due to this acoustic feedback, the flow has a very deterministic character. This is illustrated by the existence of peaks in the power spectra measured by pressure sensors or by a hot wire inserted in the mixing layer. The presence of coherent structures is observed in the mixing layer for a very wide range of Mach numbers (Cattafesta et al., 1997, McGregor and White, 1970). The number of these structures varies with the Strouhal number constructed on the oscillation frequency, the cavity length and the external velocity. The velocity field can then be broken down into a steady average, a "coherent" part related to the discrete component of the structures and a random fluctuating part. This introduces the following triple decomposition (Hussain and Reynolds, 1972):

$$u(\underline{x},t) = \bar{u}(\underline{x}) + \tilde{u}(\underline{x},t) + u'(\underline{x},t)$$

where $\bar{u}(\underline{x})$ is the average velocity component, $\tilde{u}(\underline{x},t)$ the cyclic component and $u'(\underline{x},t)$ the fluctuating component. The phase average corresponds to the term :

$$< u(\underline{x},t) >= \bar{u}(\underline{x}) + \tilde{u}(\underline{x},t)$$

It is equal to the average of u for a given phase of the flow. Because of the random nature of laser sampling, the phase average is not strictly given for a phase of the flow but instead for a fraction $\Delta\tau$ of the period. Each $\Delta\tau$ defines a class (see Lyn and Rodi, 1994).

The results of this process applied to a mixing layer developing above a deep open cavity are described for a transonic state.

EXPERIMENTAL APPARATUS

The setup is located in one of the research wind tunnels of the Fundamental and Experimental Aerodynamics Department at ONERA's Chalais-Meudon center (Jacquin et al., 1998). The stagnation conditions are ambient pressure and temperature: p_i=0.98x10^5 Pa and T_i=300 K. The wind tunnel is equipped with a constant section channel with an

area of 120x100 mm² in which the cavity is situated. The fixed Mach number of M=0.8 is controlled by means of a second motorized throat.

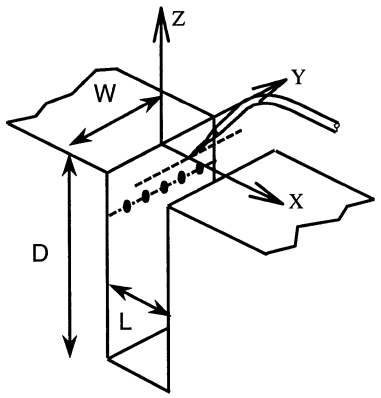

Figure 1. Schematic diagram of the cavity

The cavity length L is 50 mm and its depth D is 120 mm, giving:

$$L/D = 0.41\ ,\ L/W = 0.41\ ,\ D/W = 1$$

where W denotes the span (Figure 1). Boundary layer transition is triggered by a rough band located 200mm upstream of the trailing edge. The Reynolds number Re_{θ_0}, based on the momentum thickness θ_0 measured at the trailing edge, is equal to 7,800.

Five unsteady pressure sensors (Kulite) were installed on the upstream wall of the cavity, 35 mm below the trailing edge. The signals output by these sensors were digitized by an analog-to-digital converter (ADC) with a sample-and-hold circuit allowing simultaneous acquisition on four channels.

Rapid flow visualizations are made using a Schlieren apparatus coupled with a rotating Strobodrum type camera. Exposure is by a Nanolite spark light system controlled by a Strobokin generator. This system generates a burst of sparks with controllable frequency and duration. The burst duration is synchronized with the drum rotation to avoid overlapping of images after one revolution. The mechanical shutter is controlled manually for a long exposure time. The film used is Kodak Tmax 100 35mm film exposed at IE400. The image frequency is limited by the maximum drum rotation speed and the capabilities of the spark light (20,000 sparks per second). The combination of these two parameters sets the maximum image height on the film so that there is no overlap.

Laser Doppler Velocimeter (LDV) measurements were made using a two-component configuration. The study was made using forward scattering and the signals were processed by an IFA 750 system. The measurements were made in the median vertical plane and in the horizontal plane corresponding to the open side of the cavity. In the vertical plane, the probing mesh was finer in the mixing layer region.

DETERMINATION OF THE PHASE AVERAGES

A reference signal is required to obtain phase averages. For our reference signal, we used the central Kulite sensor located on the upstream cavity wall.

The principle of conditional laser data processing is based on their synchronization with the pressure signal. Synchronization in the present case is not an easy task because the time scales of the phenomena are very short is this transonic flow.

The pressure signal is digitized by a PC with a National Instrument EISA A2000 acquisition card operating at a maximum rate of 200 kHz per channel (1 MHz on a single channel).

The signal output of the LDV system (photomultipliers) are processed by an IFA 750 controlled by a second PC using the TSI *FIND* software. They are synchronized with the pressure signal by the ADC clock signal from the first PC. The latter is applied to a pulse counter specially designed for this experiment. The digital value corresponding to the input pulse count is encoded on two 16-bit words. This device generates two other signals to control the IFA 750: a gate signal enabling acquisition of the LDV signals by the IFA 750 and a pulse to reset the IFA 750 internal clock.

To monitor synchronization efficiency, the IFA 750 was coupled to a second device (Datalink) performing acquisition of analog or digital signals at a rate of 50 kHz. Each burst detection, the IFA 750 polls the Datalink, which sends it the last digitized data. Timing of the velocity measurements and external data is therefore synchronized with a maximum delay of 20 microseconds.

The pressure signal is connected to one of the Datalink analog inputs and the digital outputs of the pulse counter are connected to two digital inputs. This enables one to monitor synchronization of the two measurements.

CALCULATION OF THE PHASE AVERAGES

The conditioning signal (pressure) must be low-pass filtered in order to eliminate the high frequency fluctuations. This is done by means of a digital low-pass filter.

The negative component of the filtered pressure signal is first eliminated. Next, the time intervals associated with the positive values are identified. The time references corresponding to the signal maxima in these intervals are then determined and stored in a file. The velocity signal is divided into portions delimited by time references t_i and t_{i+1} determined by the above procedure. The portions are then overlaid after normalization of their duration. The resulting single period is then divided into a number of time intervals in which are stored the instantaneous velocities measured by LDV. The average velocities and Reynolds stresses are then

calculated for each interval over the entire duration of the record.

The synchronization result of the LDV and pressure measurements is illustrated in Figure 2, which shows the variation of the pressure signal digitized by the A2000 card (solid black line) and by the Datalink (symbols).

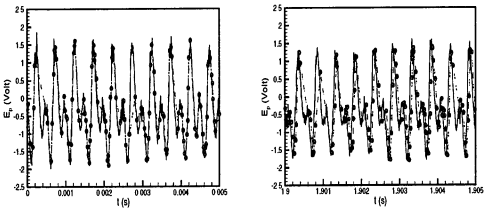

a) b)

Figure 2. LDV/Pressure Acquisition Synchronization

Each curve is plotted versus its own time base. Figure 2(a) shows the start of recording. It can be seen that the two measurements are correctly synchronized. A phase shift between the two signals can be seen in Figure 2(b) showing the end of recording. This phase shift is due to a drift between the clocks of the two acquisition systems. This drift is illustrated in Figure 3, showing the time difference t_{IFA} - t_{DI} versus time t_{DI}, where t_{IFA} is the time measured by the IFA 750 and t_{DI} is the time base of the A2000 card recorded by the Datalink.

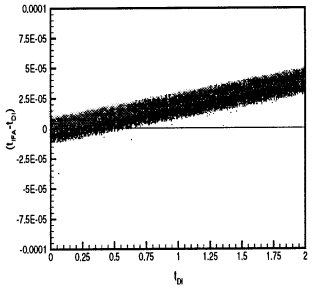

Figure 3. Drift between two systems (LDV/Pressure acquisitions)

This drift between clocks leads to a linear variation of the cloud of points on a slope of around 20µs/s. It results from a slight drift of the internal clocks of the pressure system (DI). Based on this observation, the clock drift was compensated by applying a correction coefficient to the times output by the IFA 750. This coefficient was obtained by a linear regression made on the points of Figure 3.

RESULTS

Visualizations

The frequency of the visualization system was set to its maximum, that is 20,000Hz, the frequency of the phenomenon being approximately 2,000 Hz (see below). The output films include around 200 images each. The region observed was limited to the mixing layer developing above the cavity by coupling a zoom with the Strobodrum lens. An example is shown in Figure 4. Despite the span integration performed by the Schlieren apparatus, three vortex structures are clearly visible in the mixing layer. The time sequence of the cyclic phenomenon is as follows: the first structure impinges on the downstream leading edge and penetrates the cavity. The second structure is divided into two parts, one penetrates the cavity while the other "escapes" above the downstream flat plate. The third structure, which is the least coherent, does not interact with the cavity.

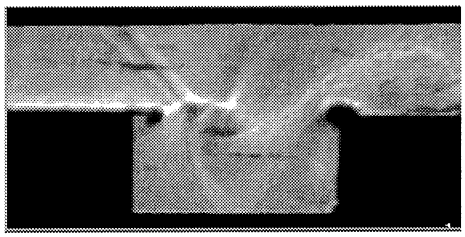

Figure 4. Schlieren picture of the mixing layer

The wavefronts which can be seen in the upper part of the image are due to reflection off the upper wall of the compression waves emanating from the leading edge (see Heller and Bliss, 1975). The presence of the dark bulb located in the downstream corner corresponds to a strong density gradient in this emission region. A pressure wave moving upstream in the internal part of the cavity can be identified in Figure 4. The convection velocity estimated from such images is around 330 m/s, i.e. close to the speed of sound in air at room temperature.

Time Averages

The maximum turbulence rate $\sqrt{\overline{u_0^{'2}}}/U_\infty$ measured in the mixing layer is 22%, where $u = \bar{u} + u_0^{'}$. A continuous initial increase of turbulent activity is observed on the $\overline{u_0^{'2}}$ profiles in the center of the mixing layer (z=0). The influence of the impingement area is characterized by appearance of a second energy peak in the lower part of the mixing layer. This phenomenon is accompanied by a reversal of the shear stress

$\overline{u_0' w_0'}$. This is due to the appearance of vertical shear in this region.

Figure 5(a) shows the mean streamlines inside the cavity.

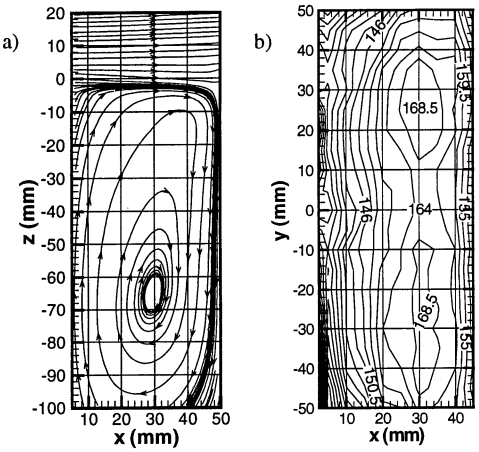

Figure 5. Mean flow characteristics

The presence of a recirculation region shifted downstream can be noted. The iso-vorticity lines (not shown here) indicate the presence of a recirculation region of opposite sign in the lower part of the cavity.

Figure 5(b) shows the isovalues of $\bar{u}$ in the z=0 horizontal plane. The velocity increases to a maximum then decreases on approaching the downstream edge of the cavity. The presence of two cells in the velocity distribution denotes a slight cellular structure. This is consistent with the observations of Maull and East (1963).

Figure 6 shows the variation of the vorticity thickness versus the downstream distance. Four regions were defined. The first two are characterized by the equation $\delta_\omega \propto 0.24x$. The third region is characterized by a steeper slope, $\delta_\omega \propto 0.48x$. The doubling of the slope value could result from a pairing process, but this is not observed in the visualizations (see below). In the fourth region, farthest downstream, the thickness no longer varies linearly. The velocity profile in similarity coordinates have been made:

$$\frac{z}{\delta_\omega} = f(\xi)$$

where

$$\xi = \frac{\bar{u}(x) - \bar{u}(x)_{\min}}{\bar{u}(x)_{\max} - \bar{u}(x)_{\min}}$$

The flow appears to be in equilibrium only in region 2. However, the initial momentum thickness evaluated from careful measurements of the initial boundary layers is $\theta_0 = 0.45mm$ which means that the above mentioned region is comprised between 30 and 50 θ_0 . This is much smaller than the required distance for a self similar regime.

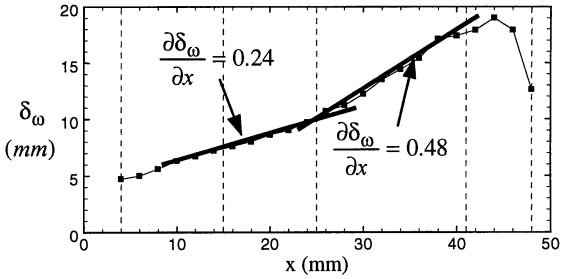

Figure 6. Axial evolution of the vorticity thickness

Phase Averages

The period of the flow oscillation was divided into twenty intervals of duration 25μs, containing an average of 2,500 samples each, with a total of 50,000 samples. The pressure signal was sampled at 200 kHz for a time equivalent to that required for acquisition of the 50,000 velocity samples.

Figure 7 shows a pressure signal sample and spectrum. The fundamental frequency (f_e) is located at 1980 Hz. There is an harmonic, lower in amplitude, at $2f_e$. The peak-to-peak amplitude of the signal corresponds to around 25% of the stagnation pressure.

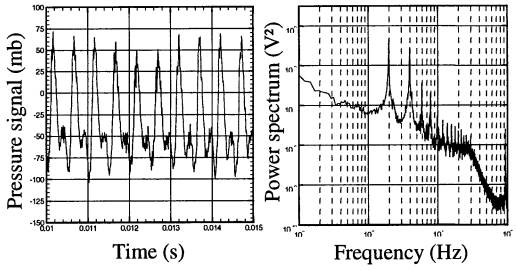

Figure 7. Pressure signal and power spectrum

Figure 8-a shows the result of the above described processing applied to longitudinal component u. The Reynolds average value (solid line) is compared with the phase average (symbols) for two separate phases. It should be noted that the phases oscillate around the average value. Strong fluctuations of the variances are observed. This clearly illustrates the major contribution of the coherent term in this type of flow. In the cross stresses (Figure c) for phase 5, a change of sign is observed at the bottom of the mixing layer near the leading edge. As mentioned above, these positive values indicate the existence of a non-negligible

mean gradient $\partial\overline{w}/\partial x$ caused by flapping of the mixing layer.

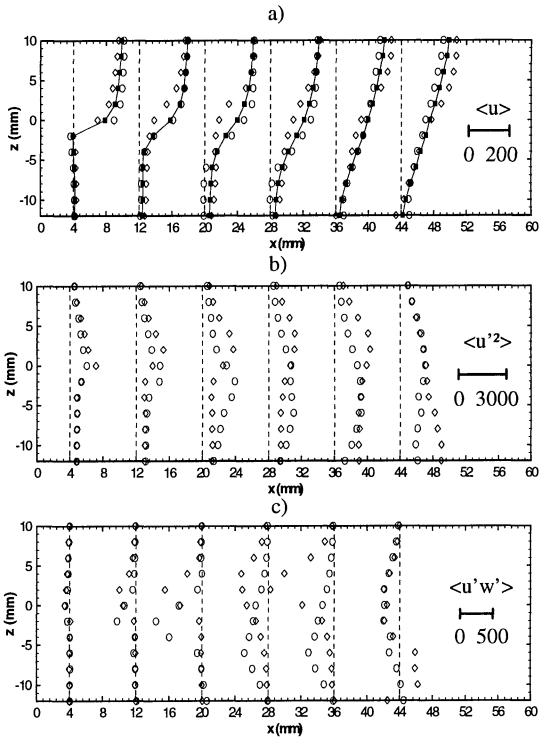

Figure 8. Phase averaged components
(◊: phase 5, o: phase 15)

This phenomenon is corroborated by analysis of the vertical mean velocity near the trailing edge of the cavity. It can be observed that phase 5 clearly corresponds to a time when the mixing layer "dips" into the cavity. Two periods can be defined. The first corresponds to positive values and the second to negative values of <w>. The two periods include roughly the same number of intervals. The small differences observed between these three curves characterize the three-dimensional nature of the flow.

For technical reasons, it was not possible to synchronize the start of acquisition of the Schlieren images with acquisition of the pressure signal. However, they were synchronized later by comparing the films with the phase averages of vorticity component $<\Omega_y>$. Figure 9 shows the comparison between the variation of the phase average of fluctuating kinetic energy $<k>$ and the visualization of a flow cycle.

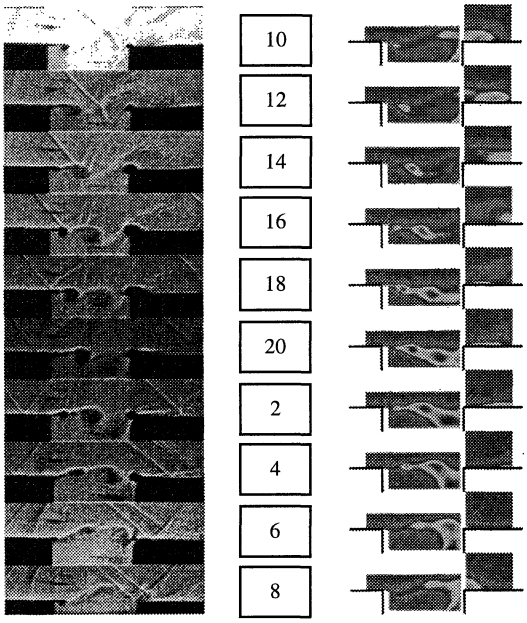

Figure 9. Phase-averaged kinetic turbulent energy vs. Fast Schlieren animation (20,000 Hz)

REMARK ON PHASE AVERAGES

One of our main concerns was to ensure satisfactory convergence of the phase averages, which explains the large number of samples in each class (2,500). It should be noted that the number of samples varies depending on the interval considered. The distribution of these samples follows the structure of the mixing layer observed in the Schlieren images. It should be noted that the rate is smaller inside the structures, probably due to centrifugation of the particles.

There is therefore a strong correlation between the coherent component $\tilde{u}$ and the number of samples per class N_i. This correlation can be quantified by the coefficient:

$$R_{\eta\tilde{u}} = \frac{\frac{1}{M}\sum_{i=1}^{M}\eta_i\tilde{u}_i}{\sqrt{\frac{1}{M}\sum_{i=1}^{M}\eta_i^2}\sqrt{\frac{1}{M}\sum_{i=1}^{M}\tilde{u}_i^2}}$$

where η_i denotes the deviation from $\overline{N_i}$ and $N_i = \overline{N_i} + \eta_i$.

This correlation introduces a large bias in the averages evaluated by direct summations on intervals. For instance, the time average of the velocity is equal to the following overall average:

$$\bar{u} = \frac{1}{N_e} \sum_{i=1}^{M} N_i < u >_i$$

where $< u >_i$ is the phase average for class *i*. Considering correlation $R_{\eta\tilde{u}}$, this average differs from that obtained by simple summing on classes:

$$<< u >>= \frac{1}{M} \sum_{i=1}^{M} < u >_i \neq \bar{u}$$

It should therefore be made sure that this inhomogeneity of the number of samples does not bias evaluation of the quantities included in the balance equations resulting from the triple breakdown. These balance equations are being evaluated.

COMPARISON BETWEEN COMPUTED AND EXPERIMENTAL DATA

One of the purposes of this work is to supply a database for validation of unsteady numerical codes. The numerical simulation must be conducted using an approach similar to that of the experiment. However, each method has its own features. For LDV signal acquisition, the sampling rate is low, random and over a time corresponding to a large number of periods (10,000 on the average). Conversely, numerical time discretization corresponds to regular sampling at high frequency, but the CPU costs sharply limit the number of periods (typically around ten). These differences must be taken into account when comparing experimental and computed results. "Degrading" the experimental results by gradually decreasing the number of periods should allow us to analyze the effect of the limited number of numerically solved periods. This should allow us to establish confidence intervals for detailed comparisons between computations and experience. This is now being done.

CONCLUSION

This communication describes the results of a study on development of a mixing layer above a cavity at transonic speed. Conditional processing of the data from a two-component LDV provides phase averages which can be used for validating L.E.S. or D.N.S. type numerical codes. Schlieren visualizations and LDV measurements are used to characterize the flapping which occurs near the downstream edge of the cavity. Limitations of the technique in this transonic application has been discussed.

To be able to make valid comparisons between computed and experimental data, it is necessary to process the numerical results in a similar way to the experimental results. A detailed analysis of the statistical processing methods required for comparison is being conducted.

ACKNOWLEDGMENTS

This work was funded by DGA/SPAé (Contract 94.34.001 BC 183).

REFERENCES

Lyn, D..A. and Rodi, W., 1994, "The Flapping Shear Layer Formed by Flow Separation from the Forward Corner of a Square Cylinder", *J. Fluid Mech*, Vol. 267, 353-376.

Sarohia, V., 1977, "Experimental Investigation of Oscillations in Flows Over Shallow Cavities", *A.I.A.A.J.*, Vol. 15, 984-991.

Rockwell, D. and Naudascher, E., 1979, "Self-Sustained Oscillations of Impinging Free Shear Layers", *Ann. Rev. Fluid Mech.*, Vol. 11, 67-94.

Powell, A., 1961, "On the edgetone", *J. Acoust. Soc. Am.*, Vol. 33, 395-409.

Rossiter, J. E., 1964, "Wind-Tunnel Experiments on the Flow Over Rectangular Cavities at Subsonic and Transonic Speeds", Reports and Memoranda No. 3438.

Cattafesta, L.N., Garg, S., Choudhari, M., and Li, F., 1997, "Active Control of Flow-Induced Cavity Resonance", A.I.A.A. Paper, 97-1804.

McGregor, O.W. and White, R. A., 1970, "Drag of Rectangular Cavities in Supersonic and Transonic Flow Inducing the Effects of Cavity Resonance", *A.I.A.A.J.*, Vol. 8, 1959-1964.

Hussain, A. K. M. F. and Reynolds, W.C., 1972, "The Mechanics of an Organized Wave in Turbulent Shear Flow, Part 2, Experimental Results", *J. Fluid Mech.*, Vol. 54, 241-261.

Jacquin, L., Forestier, N., and Geffroy P., 1998, "Caractérisation Expérimentale des Propriétés Instationnaires d'un Ecoulement au-dessus d'une Cavité Profonde en Régime Compressible (M=0,8)", ONERA Rapport Technique n°9/2496 DAFEY.

Forestier, N. Geffroy, P. and Jacquin, L., 1998, "Evaluation de Moyennes de Phase dans un Ecoulement au-dessus d'une Cavité Résonante", 6ème Congrès Francophone de Vélocimétrie Laser, ISL Saint Louis.

Heller, H. H. and Bliss, D. B., 1975, "The Physical Mechanism of Flow-Induced Pressure Fluctuations in Cavities and Concepts for their Suppression A.I.A.A. Paper , 75-491, A.I.A.A. 2nd Aero-Acoustics Conference, Hampton.

Maull, D. J. and East, L. F., 1963, "Three Dimensional Flow in Cavities", *J. Fluid Mech.*, Vol. 16, 620-632.

Bilanin, A.J. and Covert, E. E., 1973, "Estimation of Possible Excitation Frequencies for Shallow Rectangular Cavities", *A.I.A.A.J.*, Vol. 11, 347-351.

Tam, C. K. W. and Block, P. J. W., 1978, "On the Tones and Pressure Oscillations Induced by Flow Over Rectangular Cavities", *J. Fluid Mech.*, Vol. 89, 373-399.